ELSEVIER

Biophysical Chemistry 106 (2003) 31–38

Biophysical Chemistry

www.elsevier.com/locate/bpc

Interaction of $K_7Fe^{3+}P_2W_{17}O_{62}H_2$ with supported bilayer lipid membranes on platinum electrode

Jianguo Wang, Li Wang, Shaoqin Liu, Xiaojun Han, Weimin Huang, Erkang Wang*

State Kay Laboratory of Electroanalytical Chemistry, Changchun Institute of Applied Chemistry, Chinese Academy of Sciences, Changchun, Jilin 130022, PR China

Received 6 March 2003; received in revised form 2 June 2003; accepted 2 June 2003

Abstract

The influence of $K_7Fe^{3+}P_2W_{17}O_{62}H_2$ on *l*-α-phosphatidylcholine/cholesterol bilayer lipid membrane on Pt electrode was studied by voltammetry and AC impedance spectroscopy. The interaction of the polyoxometalates with the BLM can promote the access of $Ru(NH_3)_6^{3+}$ and $[Fe(CN)_6]^{3-/4-}$ to the electrode surface. It was found that some kind of pores had been formed on the BLM by AFM. The phenomenon is attributed to the interaction of $K_7Fe^{3+}P_2W_{17}O_{62}H_2$ with phosphatidylcholine phosphate groups located in its outer leaflet. Experimental results are helpful to understand the biological activity of the polyoxometalates in vivo.

Keywords: Polyoxometalates; Supported bilayer lipid membrane; Biomembrane; *l*-α-Phosphatidylcholine; Channel

1. Introduction

The bilayer lipid membrane (BLM) system has been employed extensively as an experimental model of biomembranes [1], since the reconstituted bilayer lipid membrane that separates two solutions was first reported in 1962 [2]. This biomembrane mimicking system has been mainly applied in basic research on membrane energetics and electrochemistry as well as for the purpose of biosensers and bioelectronic devices [3]. However, the major drawback of the BLM system is its instability, which limits its application for above purpose. There is a stringent demand to develop a new system that reinforces such instability without interfering with their functional aspects. In this connection, Miller introduced a simple biomembrane model which obtained by non-covalent self-organization consists of a phospholipid monolayer supported on a hanging mercury drop electrode [4]. Subsequently Nelson et al. investigated the permeability of heavy-metal ions in a modified version [5,6]. Tien et al. developed a new method of making stable BLM on freshly formed surface of hydrophilic metal such as Pt, Au, Ag, Cu, Ni or stainless steel, which is abbreviated to s-BLM [7,8]. The s-BLM possesses a high electromechanical stability, making it attractive for bioelectronic and biotechnological applications. It has been used for a number of practical applications, including immobilizing a host of compounds such as,

*Corresponding author: Tel.: +86-431-568-971-1; fax: +86-431-568-971-1.

E-mail address: ekwang@ciac.jl.cn (E. Wang).

0301-4622/03/$ - see front matter © 2003 Elsevier Science B.V. All rights reserved.
doi:10.1016/S0301-4622(03)00158-3

enzymes, antibodies, protein complex, ionophores [9–12], etc.

Polyoxometalates attract current attention in view of their potential application in catalysis, materials and medicine [13–18]. It was discovered heptamolybdates as a new type of antitumor substance, especially hexakis(isopropylammonium) heptamolybdate(VI) trihydrate $[NH_3Pr^i]_6[Mo_7O_{24}]\cdot 3H_2O$ (PM-8) which inhibits 80% of the tumor growth in mice bearing methylcholanthrene induced tumor (Meth A sarcoma) and MM-46 adenocarinoma [19]. It was found to have promising antitumor activity in vitro for organotitanium substituted heteropolytungstosilicates [20] and cyclopentadienyltitanium substtued polyoxotungstate—$[CoW_{11}O_{39}(C_pTi)]^{7-}$ ($C_p = \eta^5-C_5H_5$) for example Ref. [21]. In addition, 21-tungsto-9-antimonate $[Sb_9W_{21}O_{86}]^{-19}$ has been investigated as an acquired immunodeficiency syndrome (AIDS) antiviral drug, inhibiting the reverse transcriptase of both lymphocytopathic retrovirus and simian AIDS virus [19]. Although the biological properties of polyoxometalates have been researched considerably, there is little information on its effect on the transportation of biomembranes. The s-BLM is a useful model for understanding the effect of polyoxometalates on biological cell membranes.

In this paper, we are presently investigating the effect of polyoxometalates on cell membrane model. The current study was undertaken in an attempt to better understand the molecular mechanism of the interaction of polyoxometalates with cell membranes. In this work we present the first evidence for the interaction between s-BLM and polyoxometalates. By means of self-assembly of lipid, we made layers of lipid and cholesterol on the surface of a Pt electrode. From electrochemical AC impedance and cyclic voltammetric experiments, we induced that s-BLM has been formed. $K_7Fe^{3+}P_2W_{17}O_{62}H_2$, an aqueous-soluble potassium salt can be dissolved at pH 4.0–5.5 solution near physiological pH. It is a monosubstituted Dawson anion and an iron–porphyrin-similar compound. We found that it interacted with lipid membrane strongly and the action made $Fe(CN)_6^{3-/4-}$ and $Ru(NH_3)_6^{3-/2-}$ easy to reach the Pt electrode. Our results show that $K_7Fe^{3+}P_2W_{17}O_{62}H_2$ has a biological activity in vitro, which enhanced the transportation of the lipid membranes.

2. Experimental

2.1. Reagents

l-α-Phosphatidylcholine from fresh egg yolk was purchased from Sigma (USA). Hexaammineruthenlum(III) chloride was purchased from Aldrich Chem. Co. (USA). Cholesterol was purchased from the chemicals department of Guangzhou Medicament Company (Guangzhou, China). $K_7Fe^{3+}P_2W_{17}O_{62}H_2$ was synthesized in our laboratory according to Ref. [22]. Other chemicals were of the highest quality as possible as obtained and all chemicals were used without further purification. Obtained by means of a Millipore Q (USA) water purification set, pure water was used throughout .

2.2. Apparatus

All cyclic voltammetric experiments were carried out with a model CS-1087 Cypress Systems (Inc., Lawrence, KS, USA) connected a PC for control and data storage. The apparatus used for electrochemical impedance measurement was composed of Autolab with potentiostat/galvanostat PGSTA30 and the Frequency Response Analysis System Software (FRA) (Eco Chemie B.V. Utrecht, The Netherlands), to provide fully computer controlled electrochemical impedance spectroscopy. Impedance measurement was performed in the frequency range from 0.1 to 10000 Hz with a signal amplitude 5 mV. A standard three-electrode cell was employed for the electrochemical experiment. A platinum electrode was used as the substrate electrode and the counter electrode is a platinum wire. All potentials reported in the paper are referenced to a Ag/AgCl (KCl saturated) electrode.

Impedance measurement was performed in the presence of a 1.0 mmol l^{-1} $K_3[Fe(CN)_6]$/$K_4[Fe(CN)_6]$ (1:1) mixture containing 0.1 mol l^{-1} KCl as a redox probe at the potential of the system, $E^\circ = 319$ mV. All experiments were carried

out at room temperature. The buffer and sample solution were deaerated with purified nitrogen for 5 min at least for removing oxygen prior to the beginning of a series of experiments.

2.3. Method for supported lipid layer formation

l-α-Phosphatidylcholine (PC) and cholesterol (CH) were dissolved in heptane, giving a final concentration of 20 mg/ml PC and 7 mg/ml CH. The supported bilayer lipid membrane on a Pt electrode (diameter 1.0 mm) was first polished with sand paper, followed by alumina slurry of 1.0, 0.3, 0.05 μm on polishing cloth with water as the lubricant, respectively, then sonicated in pure water both for 2 min, rinsed with pure water, last the Pt electrode was put in the solution of 1.0 mol l^{-1} H_2SO_4. Cyclic voltammetry was performed until the characteristic of Pt was observed. The Pt electrode was immediately taken out, rinsed with pure water again and sonicated with a high power supersonic wave generator in water bath and acetone bath for 5 min, respectively. A drop of BLM forming solution was added to the surface of the Pt electrode, afterwards the electrode was rapidly transferred into the 0.1 mol l^{-1} solution, in which the supported lipid layer was formed spontaneously by self-assembly [11].

2.4. AFM experiments

l-α-Phosphatidylcholine (PC) was dissolved in chloroform to give a final concentration of 2.5 mg ml^{-1}. An aliquot droplet of the PC solution was applied to cover the surface of a freshly cleaved mica. The mica was immediately transferred into the 0.1 mol l^{-1} KCl solution for 20 min, where the supported bilayer lipid membrane was formed spontaneously. The extra PC and salts were removed with ultrapure water and blown dry with a nitrogen stream.

Surface images were acquired in tapping mode under ambient conditions (Nanoscope IIIa; Digital instruments, Inc.) Single beam silicon cantilevers (Model TESP) with spring constant in the 25–50 N/m range were used. All images, which were obtained reproducibly several times with different samples and tips, were recorded by oscillating the cantilever slightly below its resonance frequency (typically, 250–350 kHz) and raster scanning across the surface with scan rate of 1.0 Hz.

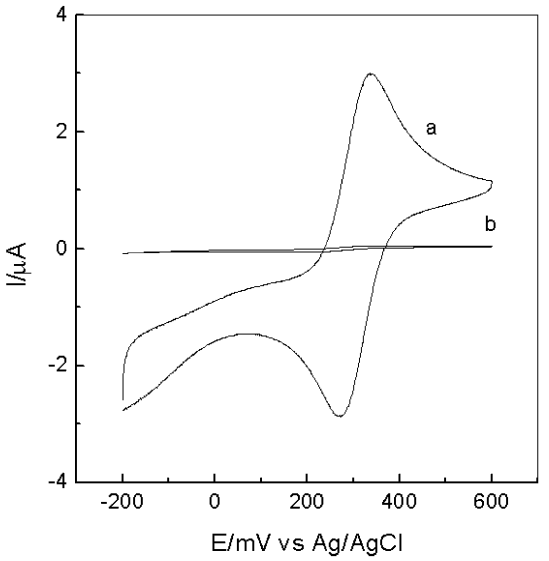

Fig. 1. Cyclic voltammetric responses of (a) at bare Pt electrode, (b) Pt electrode supported bilayer lipid membrane in 1.0 mmol l^{-1} $K_3[Fe(CN)_6]/K_4[Fe(CN)_6]$ (1:1) mixture containing 0.1 mol l^{-1} KCl. Scan rate 20 mV s^{-1}.

3. Results and discussion

3.1. Voltammetric behavior of the Pt electrode and the Pt electrode coated with lipid membrane

The cyclic voltammograms allow one to conclude if bilayer lipid membranes are of high quality. Fig. 1 shows the cyclic voltammetic response of (a) the bare Pt electrode and (b) the Pt electrode coated with supported bilayer lipid membranes in 1.0 mmol l^{-1} $K_3[Fe(CN)_6]/K_4[Fe(CN)_6]$ (1:1) solution containing 0.1 mol l^{-1} KCl. The scan rate was in the positive direction at 20 mV s^{-1}. Fig. 1a shows the redox process of ferrocyanide/ferricyanide on the bare Pt electrode. It was observed that the peak separation ΔE_{pac} was 62 mV at scan rate 20 mV s^{-1}. The data for Pt electrode are consistent with a reversible electron-transfer model. Comparing Fig. 1b with Fig. 1a, we could find a noticeable decrease in the current

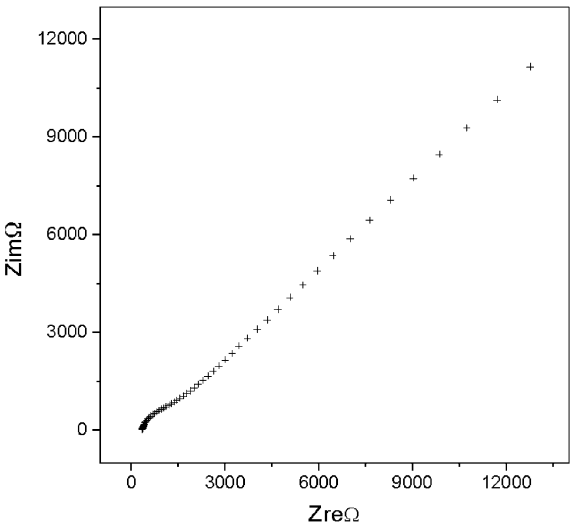

Fig. 2. Impedance spectra of bare Pt electrode in 1.0 mmol l^{-1} $K_3[Fe(CN)_6]/K_4[Fe(CN)_6]$ (1:1) mixture containing 0.1 mol l^{-1} KCl.

response of the electrode and an increase in the peak-to-peak separation between the cathodic and anodic waves of $K_3[Fe(CN)_6]/K_4[Fe(CN)_6]$. It means that $[Fe(CN)_6]^{3-/4-}$ was prevented from reaching the surface of Pt electrode. Hence, it is clear that the supported lipid membranes had been formed on the surface of Pt electrode successfully.

3.2. Impedance measurement of the Pt electrode supported lipid membranes

The experimentally obtained impedance data for a given electrode interface may be analyzed by an exact mathematical model that predicts the theoretical impedance $Z(w)$, or by a relatively equivalent circuit consisting of ideal and non-ideal electrical analogs to the real physical and chemical processes [23]. The latter approach was used in the present work. Impedance data were fitted to an equivalent circuit using FRA. One of the objectives of the present study was to define and discuss the analogies between circuit elements and electrochemical processes, so that the result of data fitting can conclude more easily the features of a surface-modified electrode. The complex impedance can be presented as the sum of the real, Z_{re} and imaginary, Z_{im} components that originate mainly from the resistance and capacitance of the cell, respectively.

Fig. 2 illustrates the result of impedance spectroscopy on a bare Pt electrode in the presence of equimolar 1.0 mmol l^{-1} $[Fe(CN)_6]^{3-/4-}$ and 0.1 mol l^{-1} KCl solution, which are measured at the formal potential of $[Fe(CN)_6]^{3-/4-}$. The very small semicircle located near the origin is probed by higher frequencies than the linear region located to the right in plot A. It means that in higher frequency range the dynamics of electron transfer is observed in the impedance spectroscopy experiment and the current due to voltage excitation is under kinetic control. The low-frequency region of plot A, where the slope of Z_{re} vs. Z_{im} is unity, is dominated by mass transfer of the redox species to and from the interfacial region.

Fig. 3 shows the impedance spectra of Pt electrode with supported lipid membrane. It is known that the capacity of polycrystalline gold electrode shows a marked dependence or constant phase element (CPE) [24]. The phenomenon is attributed

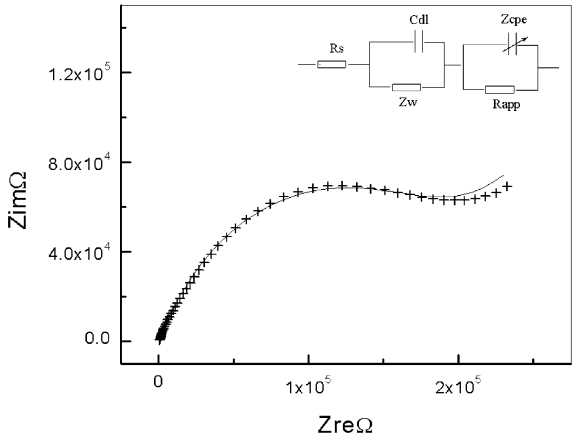

Fig. 3. Impedance spectra (+) of Pt electrode supported bilayer lipid membranes in 1.0 mmol l^{-1} $K_3[Fe(CN)_6]/K_4[Fe(CN)_6]$ (1:1) mixture containing 0.1 mol l^{-1} KCl. Fit to the spectra is indicated by the solid line. Inset shows the equivalent circuit, consisting of the solution resistance R_s, in series with two paralleled circuits, with one composed of the double-layer capacitance C_{dl}, Warburg impedance Z_w, and the other the membrane capacitance related constant-phase element impedance Z_{cpe}, the apparent charge transfer resistance R_{app}.

to surface inhomogeneity [25] and the effect would be observed as a depressed semicircle in the complex plane. On the other hand, the membrane is a lipid bilayer with hydrophilic groups on the surface and hydrophobic hydrocarbon chains inside. The change of dipolar direction may affect the orientation of hydrophobic chains with respect to the metal surface, causing them to fluctuate from perpendicular to surface (motion) to lean against the surface (touch), thus resulting in the change of the membrane thickness. It is known that the capacitanae C_m depends on the membrane thickness as following relation:

$$C_m = \varepsilon\varepsilon_o/d$$

where d is the thickness of s-BLM, ε is the relative dielectric permittivity of the lipid, ε_o is the dielectric permittivity of the free space. While under high frequency, the fluctuation of modulated potential is so fast that the hydrocarbon chains could not react in time, as a result, the thickness of the membrane remains stable, and so does the membrane capacitance [26]. It can also be seen that the average value of C_m decreases with the increase of frequency, as reported by others [27,28]. The CPE effect was also verified in the present experiments, hence, the interface could not be represented as a simple capacitor in an equivalent circuit representation. The equivalent circuit adopted to model the Pt-BLM system in the above-mentioned solutions was presented in Fig. 3. The impedance of the system is represented by the solution resistance R_s, in series with two paralleled circuits, with one composed of the double-layer capacitance C_{dl}, Warburg impedance Z_w, and the other the membrane capacitance related constant-phase element impedance Z_{cpe}, the apparent charge transfer resistance R_{app}. A constant-phase element Z_{cpe} is used instead of a membrane capacitance in the equivalent circuit. For the constant-phase impedance [29]:

$$Z_{cpe}^{-1} = C_m(j\omega)^{\alpha}$$

Where the value of membrane capacitance C_m is independent of frequency, $j=(-1)^{1/2}$, and ω is the angular frequency. The exponent α is fractional

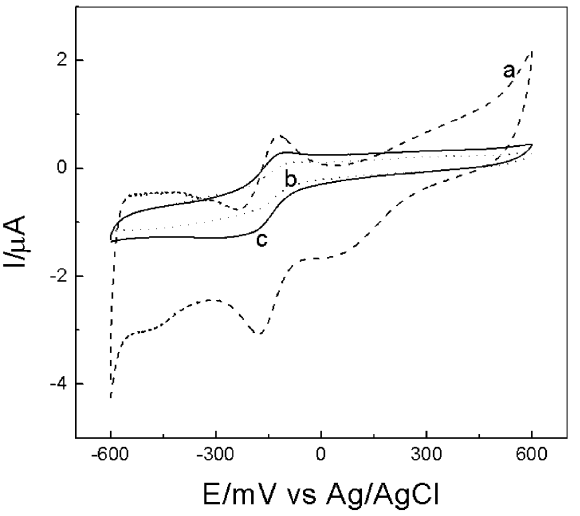

Fig. 4. Cyclic voltammetric responses of 1.0 mmol l^{-1} $Ru(NH_3)_6^{3+}$ solution containing 0.5 mol l^{-1} NaF. Scan rate 20 mV s^{-1}, (a) at bare Pt electrode, (b) at Pt electrode supported bilayer lipid membranes, (c) at Pt electrode supported bilayer lipid membranes after the interaction of 0.4 mg ml^{-1} $K_7Fe^{3+}P_2W_{17}O_{62}H_2$ with the BLM.

and its experimental value for ideally polarizable electrode is between 0.5 (for a real porous electrode) and 1 (for a perfect smooth electrode) [30]. The values of C_m, α extracted from the fit to the equivalent circuit were 0.3 $\mu F/cm^2$, 0.69, respectively. The capacitance of this membrane is somewhat lower than that of solvent-free BLMs, 0.7–0.8 $\mu F/cm^2$, thus denoting the incorporation of alkane molecules [31]. It could be concluded that a bilayer was supported on the Pt electrode.

3.3. Pores behavior of the supported bilayer lipid membranes

After the BLM was formed on the surface of Pt, the electrode was immersed in 1.0 mmol l^{-1} $Ru(NH_3)_6^{3+}$ solution containing 0.5 mol l^{-1} NaF. The cyclic voltammetric (CV) response of the electrode was recorded as Fig. 4a. Fig. 4b shows the CV response of the bare Pt electrode in 1.0 mmol l^{-1} $Ru(NH_3)_6^{3+}$ solution containing 0.5 mol l^{-1} NaF. Comparing Fig. 4a,b, we could find a decrease in the current response of the electrode and an increase in the peak-to-peak separation

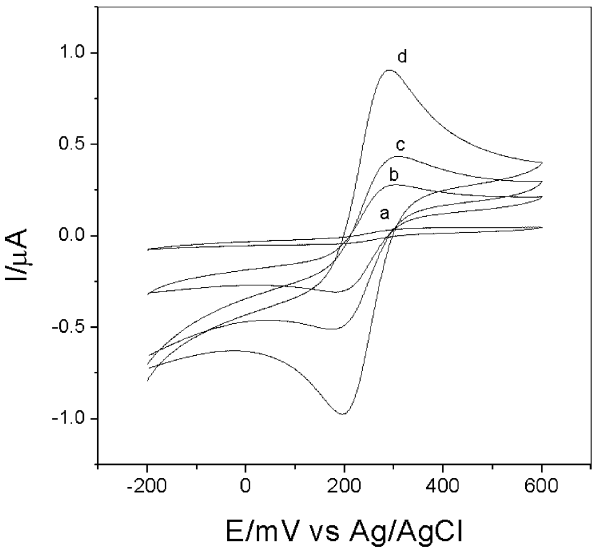

Fig. 5. Cyclic voltammetric responses of 1.0 mmol l^{-1} $K_3[Fe(CN)_6]/K_4[Fe(CN)_6]$ (1:1) mixture containing 0.1 mol l^{-1} KCl, at Pt electrode supported bilayer lipid membranes after interaction with different concentration of $K_7Fe^{3+}P_2V_{17}O_{62}H_2$: (a) 0, (b) 0.2, (c) 0.42, (d) 0.80 mg ml^{-1}, Scan rate 20 mV s^{-1}.

between the cathodic and anodic waves of $Ru(NH_3)_6^{3+}$. We attributed the changes to the obstacle of the lipid membranes, because the presence of the lipid bilayer membrane greatly reduces the interference and effectively exclude hydrophilic electroactive compounds to reach the detecting surface [32].

When we put the electrode into the solution containing 2.0 mg ml^{-1} $K_7Fe^{3+}P_2W_{17}O_{62}H_2$ and 0.2 mol l^{-1} acetate (pH5.06) for 60 min, then took out it, immersed it in 1.0 mmol l^{-1} $Ru(NH_3)_6^{3+}$ solution containing 0.5 mol l^{-1} NaF. Its CV response was recorded as Fig. 4c. A distinct CV response from the ruthenium(II) complex cation was gained as if the lipid membranes were 'leaking'. It means that the effective electrode area was increased. It can be known that $K_7Fe^{3+}P_2W_{17}O_{62}H_2$ induce some active sites on the BLM and $Ru(NH_3)_6^{3+}$ can diffuse across the s-BLM at the active sites, which we call pores. Although $K_7Fe^{3+}P_2W_{17}O_{62}H_2$ is charged negatively and repel $Fe(CN)_6^{3-/4-}$, $Fe(CN)_6^{3-/4-}$ can also diffuse through the channel, its CV response is shown as Fig. 5. The reasonable explanations are (a) the $K_7Fe^{3+}P_2W_{17}O_{62}H_2$ is not simply adsorbed on the s-BLM surface, it interacts with s-BLM and produces some pores. The pores do not have selectivity so that $Ru(NH_3)_6^{3+}$ and $Fe(CN)_6^{3-/4-}$ can reach the surface of electrode and produce CV response. (b) The density of $K_7Fe^{3+}P_2W_{17}O_{62}H_2$ charged is comparatively low so that $Fe(CN)_6^{3-/4-}$ can diffuse and reach the surface of the electrode like $Ru(NH_3)_6^{3+}$.

With the presence of $K_7Fe^{3+}P_2W_{17}O_{62}H_2$ as stimulus and $Fe(CN)_6^{3-/4-}$ as the marker ion, the cyclic voltammetric response of the s-BLM with different concentrations of $K_7Fe^{3+}P_2W_{17}O_{62}H_2$ was tested. The intensity of the peak current increased with the concentration of $K_7Fe^{3+}P_2W_{17}O_{62}H_2$ (Fig. 5). This can be attributed to higher concentration of $K_7Fe^{3+}P_2W_{17}O_{62}H_2$ producing more pores, so it causes more $Fe(CN)_6^{3-/4-}$ reach the surface of the electrode. Furthermore, the pore behavior is time-dependent. Fig. 6 shows the current response of the channel as a function of time. The peak current of $Fe(CN)_6^{3-/4-}$ increased with time and reached steady state after 120 min. We took out the

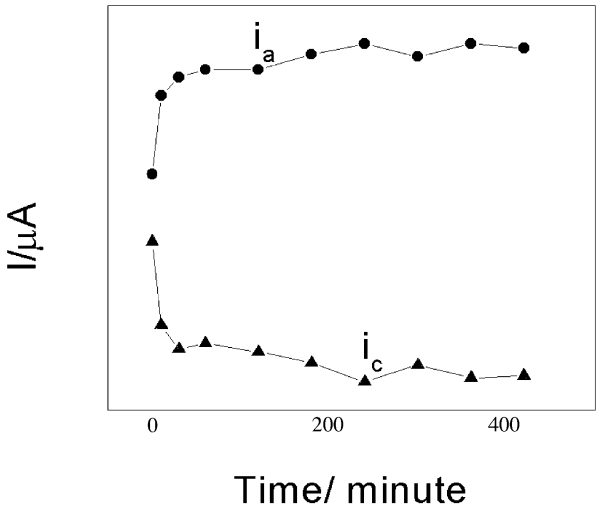

Fig. 6. Cathodic and anodic peak currents of 1.0 mmol l^{-1} $K_3[Fe(CN)_6]/K_4[Fe(CN)_6]$ (1:1) mixture containing 0.1 mol l^{-1} KCl, at Pt electrode supported bilayer lipid membranes as a function of time after interaction with 0.80 mg ml^{-1} $K_7Fe^{3+}P_2W_{17}O_{62}H_2$, Scan rate 20 mV s^{-1}.

electrode and then immersed it in the solution containing 0.2 mol l^{-1} acetate (pH 5.06) and found the pore behavior was kept stable more than 10 h. It was concluded that the bond between $K_7Fe^{3+}P_2W_{17}O_{62}H_2$ and lipid was firm.

Atomic force microscopy (AFM) has proven to be a useful method to elucidate the structure of supported phospholipid bilayer during the last decade [33]. It was employed to investigate the changes of surface image of BLM here. Fig. 7a shows the PC film formed on freshly cleaved mica, it is a smooth and flat film. The same PC/BLM film was used in experiments to interact with polyoxometalates, and the AFM image was shown in Fig. 7b. It was obvious that after the interaction with polyoxometalates, the surface image of the PC film had some changes. Some bumps were shown in the image, which were particles of polyoxometalates attracted to the lipid film. There were also a few new defects and pores formed on the surface of BLM, which caused the promotion of the redox couples reaching the surface of electrode. Thus, the polyoxometalates interacted with lipid film strongly, and it was consistent with the electrochemistry results.

From all the above experiments, we can concluded that the interaction of $K_7Fe^{3+}P_2W_{17}O_{62}H_2$ with the s-BLM produces pores, which allow the redox couple reach to the surface of the electrode. We also investigated Cl^- and Ac^- and did not find they could induce the channels on the s-BLM. As PC is neutral, the interaction of $K_7Fe^{3+}P_2W_{17}O_{62}H_2$ with the s-BLM should not be of the electrostatic action nature. We presumed that the interaction may be $K_7Fe^{3+}P_2W_{17}O_{62}H_2$ with the head of PC, which lessens the interaction among PC head groups and between PC head and cholesterol head group like the interactions of Cu^{2+} and $Al(acac)_3$ with cell membranes and model phospholipid bilayers [34,35]. The resulting molecular arrangement changes loose, even some channels were produced, which let $Ru(NH_3)_6^{3+}$ and $Fe(CN)_6^{3-/4-}$ penetrate into the s-BLM. If $K_7Fe^{3+}P_2W_{17}O_{62}H_2$ were in vivo, the interaction should affect the activity of membrane bound proteins and permeability of cell membrane. The phenomenon we observed may be helpful for us to explain that polyoxometalates inhibit the tumor growth. It is perhaps similar to the action of α-hemolysin damage human erythrocytes, α-hemolysin forms channel on the membrane of erythrocytes and leads the erythrocytes hemolysis [36,37]. Because of little volume of data, the interaction between polyoxometalates and lipid remains poorly understood. It is still premature to define the molecular mechanism of $K_7Fe^{3+}P_2W_{17}O_{62}H_2$ interaction with BLM. The subject will be understood thoroughly in future.

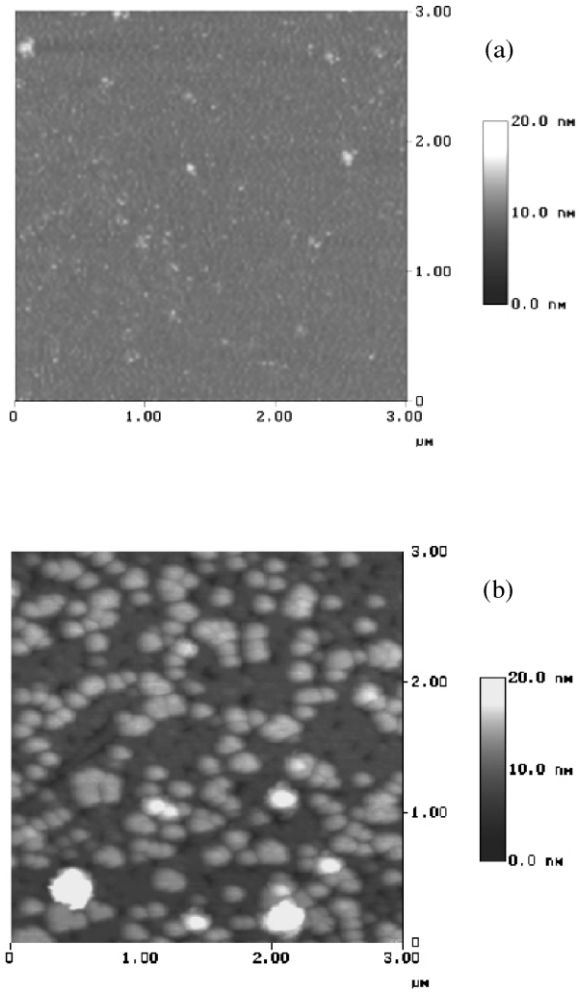

Fig. 7. (a) AFM image (scan area: 3.0×3.0 μm, vertical scale: 20 nm) of the PC films. (b) AFM image (scan area: 3.0×3.0 μm, vertical scale: 20 nm) of PC films after the interaction of 0.4 mg ml^{-1} $K_7Fe^{3+}P_2W_{17}O_{62}H_2$ with the BLM.

Acknowledgments

This work was supported by the National Natural Science Foundation of China with grant No. 29835120, 20275037.

References

[1] H.T. Tien, Bilayer lipid membranes (BLM): Theory and Practice, Marcel Dekker, New York, 1974.
[2] P. Muller, D.O. Rudin, H.T. Tien, W.C. Wescott, Nature 194 (1962) 979.
[3] K. Pawel, B.-S. Maria, Bioelectroch. Bioener. 44 (1998) 163.
[4] I.R. Miller, in: G. Milazzo (Ed.), Topics in Bioelectrochemistry and Bioenergetics, Wiley, Chichester, 1981, pp. 177–180.
[5] A. Nelson, J. Chem. Soc. Faraday Trans. 87 (12) (1991) 1851.
[6] A. Nelson, H.P. van Leeuwen, J. Electroanal. Chem. 273 (1989) 183.
[7] A. Wardak, H.T. Tien, Bioelectroch. Bioener. 24 (1990) 1.
[8] T. Martynski, H.T. Tien, Bioelectroch. Bioener. 25 (1991) 317.
[9] J.D. Burgess, M.C. Rhoten, M. Hawkridge, Langmuir 14 (1998) 2467.
[10] S. Schouten, P. Stroeve, M.L. Longo, Langmuir 5 (1999) 8133.
[11] D.-L. Jiang, P. Diao, R.-T. Tong, D.-P. Gu, B. Zhong, Bioelectroch. Bioener. 44 (1998) 285.
[12] M. Liley, J. Bouvier, H. Vogel, J. Colloid Interf. Sci. 194 (1997) 53.
[13] G.M. Kloster, F.C. Anson, Electrochim. Acta 44 (1999) 2271.
[14] A. Kuhn, N. Mano, C. Vidal, J. Electroanal. Chem. 463 (1999) 187.
[15] M. Barth, M. Lapkowski, S. Lefrant, Electrochim. Acta 44 (1999) 2117.
[16] W.-B. Song, Y. Liu, N. Lu, H.-D. Xu, C.-Q. Sun, Electrochim. Acta 45 (2000) 1639.
[17] M.E. Tess, J.A. Cox, Electroanalytical 10 (1998) 1237.
[18] B. Keita, K. Essaadi, L. Nadjo, M. Desmadril, Chem. Phys. Lett. 237 (1995) 411–418.
[19] T. Yamase, Inorg. Chim. Acta 151 (1988) 15.
[20] X.-H. Wang, Z.-G. Sun, J.-F. Liu, Chinese J. Chem. 17 (1999) 526.
[21] X.-H. Wang, J.-F. Liu, J.-X. Li, Y. Yang, J.-T. Liu, B. Li, M.T. Pope, J. Inorg. Biochem. 94 (2003) 279.
[22] D.K. Lyon, W.K. Miller, T. Novet, P.J. Domaille, E. Evitt, D.C. Johnson, R.G. Finke, J. Am. Chem. Soc. 113 (1991) 7209.
[23] L.V. Protsailo, W.R. Fawcett, Electrochim. Acta 45 (2000) 3497.
[24] W.R. Fawcett, Z. Kovacova, A.J. Motheo, C.A. Foss Jr, J. Electroanal. Chem. 326 (1992) 91.
[25] W. Schelder, J. Phys. Chem. 79 (1975) 127.
[26] H. Gao, J. Feng, G.-A. Luo, A.L. Ottova, H.T. Tien, Electroanalytical 13 (2001) 49.
[27] J. Sabo, A. Ottova, G. Laputkova, M. Legin, L. Vojcikova, H.T. Tien, Thin Solid Films 306 (1997) 112.
[28] V.I. Passeclmik, T. Hianik, S.A. Ivoanov, B. Sivak, Electroanalytical 10 (1998) 295.
[29] S. Ye, F. Girard, D. Belanger, J. Phys. Chem. 97 (1993) 12373.
[30] P. Diao, D. Jiang, X. Cui, D. Gu, R. Tong, B. Zhong, Bioelectroch. Bioener. 45 (1998) 173.
[31] R. Guidelli, G. Aloisi, L. Becucci, A. Dolfi, M.R. Moncelli, F.T. Buoninsegni, J. Electroanal. Chem. 504 (2001) 1.
[32] H.T. Tien, A.L. Ottova, Electrochim. Acta 43 (1998) 3598.
[33] Y.F. Dufrene, G.U. Lee, Biochimica et Biophysica Acta 1509 (2000) 14.
[34] M. Suwalsky, B. Ungerer, L. Quevedo, F. Aguilar, C.P. Sotomayor, J. Inorg. Biochem. 70 (1998) 233.
[35] M. Suwalsky, B. Ungerer, F. Villena, B. Norris, H. Cardenas, P. Zatta, J. Inorg. Biochem. 75 (1999) 263.
[36] L.-Z. Song, M.R. Hobaugh, C. Shustak, S. Chekey, H. Bayley, J.E. Gouaux, Science 274 (1996) 1859.
[37] H. Bayley, Sci. Am. 277 (3) (1997) 62.